



Faculty of Informatics
Masaryk University

Object Tracking in Bioimage Data

Habilitation Thesis
(Collection of Articles)

Martin Maška

April 2020

Abstract

Object tracking plays an important role in understanding the principles of intracellular and intercellular processes, with particles, cells, and cell membrane protrusions being typical targets of interest. Subsequent downstream analyses of their spatiotemporal lineages help to quantitatively characterize their migratory patterns, morphological changes, or mutual interactions and relationships, with the primary aim of revealing novel insights on the behavior of these targets under different physiological and pathological conditions. The advances in optical microscopy and fluorescent reporters have facilitated observations of these targets at unprecedented spatiotemporal resolutions, at the expense of acquiring massive amounts of bioimage data, calling for robust and automatic bioimage analysis workflows to substitute for subjective, highly error-prone, and extremely laborious manual analyses.

In this thesis, the author surveys his concerted efforts made to develop robust and fully automatic workflows for tracking particles, cells, and filopodial protrusions in multidimensional bioimage data. This involves not only novel algorithmic contributions, but also establishing of heterogeneous benchmark datasets and rigorous evaluation protocols to identify the limits and to assess the parameter sensitivity of these workflows. The thesis is structured as a comprehensive commentary to a selected collection of three conference papers and nine journal articles, highlighting the most important results achieved and their contributions to the state of the art.

Acknowledgments

First of all, the author would like to express his gratitude to Pavel Matula, Petr Matula, Michal Kozubek, Carlos Ortiz de Solórzano, and Arrate Muñoz-Barrutia who all were his mentors on the way to becoming a scientist. Special thanks also go to individual co-authors of the papers included in this collection and to other colleagues and collaborators for fruitful discussions and open-mindedness. Last but not least, the author thanks his family for their patience and love.

Contents

I	Commentary	1
1	Introduction	3
2	Particle Tracking	5
3	Cell Tracking	9
4	Filopodium Tracking	15
5	Conclusion	19
	Bibliography	21

Part I

Commentary

Chapter 1

Introduction

The state-of-the-art bioimaging instruments routinely produce multidimensional bioimage data of enormous quantities [42], calling for robust and automatic bioimage analysis workflows to substitute for subjective, highly error-prone, and extremely laborious manual analyses [15, 40, 7]. Object tracking is instrumental in understanding the principles of various intracellular and intercellular processes, with particles, cells, and cell membrane protrusions being common targets of interest [52, 16, 21]. The spatiotemporal lineages produced by bioimage object trackers form the solid ground for subsequent downstream analyses that shed more light on migratory patterns, morphological changes, and mutual interactions and relationships of the targets under investigation, thus providing important clues on their behavior in both tissue development and disease [1, 41, 22]. Unsurprisingly, the truly informative and unbiased value of such conclusions highly depends on the correctness of image analysis results and their possible curation. Therefore, there has been an increasing demand for evaluating bioimage analysis workflows to objectively assess their performance [25], leading to the boom in organizing biomedical competitions [14, 39, 49, 58, 50, 7], which in turn has called for control mechanisms and best practices to guarantee their fairness [32, 48], and also for publicly available repositories of heterogeneous, annotated bioimage data. To this end, image-based simulations [59], allowing straightforward in-depth performance assessments due to the inherent availability of complete reference annotations and natural capability of generating bioimage data of the same targets of interest under varying environmental and imaging setups, have greatly been exploited [14, 39, 49, 58, 50].

Purpose and focus of the thesis

The primary objective of this thesis is to comprehensively summarize the author's main algorithmic contributions as well as benchmarking efforts toward developing robust and automatic workflows for tracking particles, cells, and filopodial protrusions in multidimensional bioimage data. This is a research topic he has been attending to since receiving his Ph.D. in 2011 on segmenting fluorescent cells using fast level set-like algorithms. Apart from co-organizing two renowned competitions, Particle Tracking Challenge and Cell Tracking Challenge, that evolved into publicly available benchmarks for objective comparison of particle and cell tracking methods [14, 39, 58], the author was awarded a three-year grant from the Czech Science Foundation on tracking filopodial cells and received the Masaryk University Rector's Award for Outstanding Research Results Achieved by Young Scientists under 35 in 2016. As of April 2020, he has

co-authored 18 publications on object tracking in bioimage data, with more than 500 citations received according to the Web of Science database. Their representative subset, consisting of three conference papers and nine journal articles, is included in this thesis and is accompanied by a comprehensive commentary, highlighting the most important results achieved and their contributions to the state of the art.

Structure of the thesis

In the following three chapters, the state of the art of particle tracking (Chapter 2), cell tracking (Chapter 3), and filopodium tracking (Chapter 4) is briefly surveyed, being complemented with the author's contributions and with the lists of co-authored, representative papers relevant to individual tracking tasks. Finally, a short personal perspective on some of the actual research gaps and possible near-future research directions toward their addressing is presented in Chapter 5. In case of the printed version of the thesis, all selected papers in the collection are attached. However, they are purposely excluded from an online, publicly available version of the thesis to avoid copyright infringement.

Chapter 2

Particle Tracking

Particle tracking is of fundamental importance in diverse quantitative analyses of dynamic intracellular processes using time-lapse microscopy [52]. The particle can be anything from a single molecule to a macromolecular complex, organelle, virus, or microsphere manifesting itself as a small dot in the image data. The problem of particle tracking can be formulated as having a recorded time-lapse sequence of moving dot-like objects, one is interested in spatiotemporal positions of individual objects. Due to the frequent impracticability of tracking particles manually, a number of fully automatic particle trackers have been developed over past decades [29], carrying out the tracking task in two subsequent phases: (1) particle detection and (2) particle linking. First, individual particles are detected separately in every frame of a given time-lapse sequence. Second, the detected particles are linked into tracks, a set of which forms a linear oriented forest (LOF) in the terminology of graph theory. Common approaches to particle detection range from simple thresholding or local-maxima finding to more advanced linear and nonlinear model fitting and centroid estimation schemes, whereas the linking of detected particles ranges from simple nearest-neighbor to multiframe association with or without the explicit guidance derived from motion models and state estimation [23, 41, 12, 13, 19, 30, 51]. In line with the widespread use of deep learning across different computer vision and bioimage analysis tasks [26, 42], the self-learning capabilities of deep neural networks have also been exploited for both particle detection [43, 62] as well as particle linking [63, 54] over recent years.

Contributions

Bearing calls for open science [8] and reproducible research [9] in mind, the author co-organized the Particle Tracking Challenge (PTC, <http://bioimageanalysis.org/track/>) in collaboration with the Biomedical Imaging Group Rotterdam (Erasmus University Medical Center, the Netherlands) and Quantitative Image Analysis Unit (Institut Pasteur, France). By gathering the bioimage informatics community and coordinating an open competition hosted by the 2012 IEEE International Symposium on Biomedical Imaging, the challenge organizers established a novel benchmark for objective and systematic comparison of particle tracking algorithms [14]. Using a completely annotated repository of computer-generated image data, consisting of four biologically driven scenarios with various particle appearance, dynamics, density, and signal (Fig. 2.1), and a diverse set of performance evaluation criteria, 14 particle trackers were objectively compared and clear differences between them, leading to important practical conclusions

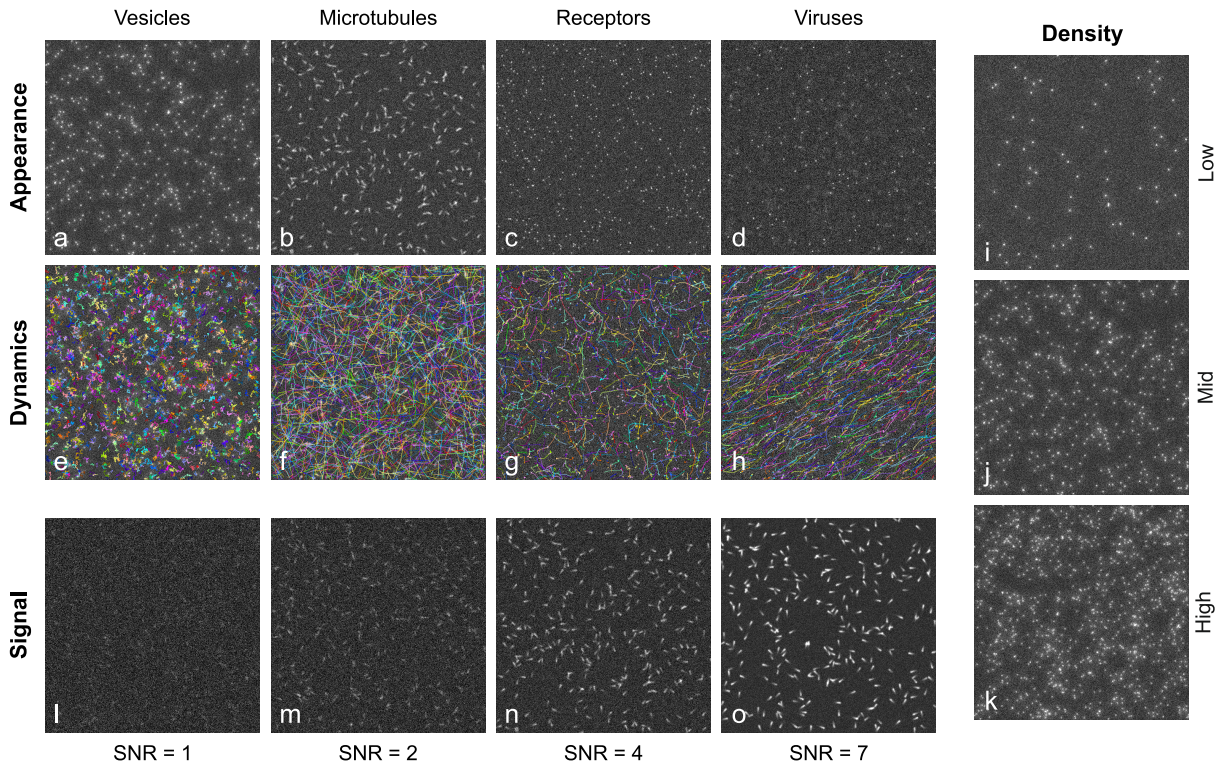


Figure 2.1: Samples of the Particle Tracking Challenge image data, with varying particle (a-d) appearance, (e-h) dynamics, (i-k) density, and (l-o) signal. The figure was reproduced from [14].

for developers and users, were revealed. As of April 2020, this has been demonstrated not only by receiving more than 250 citations according to the Web of Science database and by tagging the paper as highly cited there, but also by continually exploiting the PTC dataset repository for further algorithmic improvements [30, 63, 54, 62].

Subsequent in-depth analyses of the PTC evaluation protocol revealed that its performance assessment strongly depends on the algorithm linking capabilities [36]. Indeed, it establishes particle correspondences at the level of individual tracks, and thus produces possibly inconsistent scoring for identical configurations of tracking errors with different temporal contexts. Furthermore, it provides neither users nor developers with any direct information about individual linking errors committed by the algorithm, which may complicate its parameter fine-tuning and further algorithmic developments. To address these difficulties, we developed a new evaluation protocol based on the Linear Oriented Forests Matching (LOFM) measure [36]. It establishes correspondences between a reference LOF and an algorithm-generated LOF at the level of particle detections and measures the difficulty of transforming an algorithm-generated LOF to a reference LOF by normalizing a weighted sum of the lowest number of allowed graph operations needed to make both LOFs identical. The new evaluation protocol allows one to assess detection and linking performance of the algorithm in an isolated, unbiased manner, thus consistently penalizing identical, time-varying configurations of tracking errors, and to directly identify pre-defined graph operations needed to transform the algorithm-generated LOF to the reference one, thus recognizing individual tracking errors committed by the algorithm. By re-

Scenario	Density	SNR	Microtubules						Receptors						Vesicles						Viruses					
			Low		Mid		High		Low		Mid		High		Low		Mid		High		Low		Mid		High	
			4	7	4	7	4	7	4	7	4	7	4	7	4	7	4	7	4	7	4	7	4	7	4	7
Detection JSC	#1		5	2	4	2	4	2	3	3	3	3	3	3	5	7	7	7	7	7	1	1	5	1	2	2
	#2		11	4	11	4	11	4	11	11	11	11	11	11	7	3	3	3	3	1	5	5	2	2	5	5
	#3		4	5	5	11	5	11	1	1	1	9	1	1	3	5	1	1	1	5	2	2	1	5	1	1
Linking α	#1		4	4	4	4	4	4	11	11	3	3	3	3	5	1	1	1	1	1	1	1	5	2	2	2
	#2		8	5	2	2	2	2	1	1	11	11	11	11	11	8	8	8	3	5	5	5	2	1	5	5
	#3		5	2	5	5	11	5	3	8	1	5	1	1	3	5	3	3	5	8	2	2	1	5	1	1

Scenario	Density	SNR	Microtubules						Receptors						Vesicles						Viruses					
			Low		Mid		High		Low		Mid		High		Low		Mid		High		Low		Mid		High	
			4	7	4	7	4	7	4	7	4	7	4	7	4	7	4	7	4	7	4	7	4	7	4	7
Detection LOFM _b	#1		1	1	1	1	12	1	1	11	3	3	3	3	7	7	7	7	7	7	5	1	2	1	2	2
	#2		8	12	12	12	1	12	11	3	11	11	11	1	5	11	3	3	1	1	1	5	5	2	1	1
	#3		11	4	5	2	5	2	3	1	12	1	12	5	11	11	3	1	11	11	5	2	2	1	5	5
Linking LOFM _L	#1		5	4	4	4	4	4	3	3	3	3	11	11	3	3	1	1	8	7	1	1	5	5	5	2
	#2		11	2	5	2	8	2	11	11	11	11	3	3	1	1	3	3	3	1	12	5	2	1	2	5
	#3		13	5	8	11	11	11	1	9	1	8	2	1	12	12	7	7	1	2	5	8	1	8	8	8

Figure 2.2: The top three best-performing algorithms in terms of particle detection and linking according to the Particle Tracking Challenge evaluation protocol (top panel) and the Linear Oriented Forests Matching (LOFM) measure (bottom panel). The figure was reproduced from [36].

analyzing the results of all 14 particle trackers that competed in PTC, it has been shown that the LOFM-based evaluation protocol compiles substantially different rankings from those reported previously using the PTC evaluation protocol (Fig. 2.2). In addition to performance-oriented evaluation of particle trackers, the symmetric nature of established vertex correspondences allows one to use the LOFM measure also for determining differences between multiple manual annotations of point-like targets [56, 11], thus finding its application in annotation fusing too.

Articles in collection (in chronological order)

- N. Chenouard, I. Smal, F. de Chaumont, M. Maška, I. F. Sbalzarini, Y. Gong, J. Cardinale, C. Carthel, S. Coraluppi, M. Winter, A. R. Cohen, W. J. Godinez, K. Rohr, Y. Kalaidzidis, L. Liang, J. Duncan, H. Shen, Y. Xu, K. E. G. Magnusson, J. Jaldén, H. M. Blau, P. Paul-Gilloteaux, P. Roudot, C. Kervrann, F. Waharte, J.-Y. Tinevez, S. L. Shorte, J. Willemse, K. Celler, G. P. van Wezel, H.-W. Dan, Y.-S. Tsai, C. Ortiz-de-Solórzano, J.-C. Olivo-Marin, and E. Meijering. Objective comparison of particle tracking methods. *Nature Methods*, 11(3):281–289, 2014. [14]

Author’s contribution: preparation of image data; evaluation and analysis of results; paper editing

- M. Maška and P. Matula. Particle tracking accuracy measurement based on comparison of linear oriented forests. In *IEEE International Conference on Computer Vision Workshops*, pages 11–17, 2017. [36]

Author’s contribution: method design, development, and implementation; evaluation and analysis of results; paper writing

Chapter 3

Cell Tracking

Cell tracking is a key step in understanding a large variety of nontrivial biological processes [1]. Given a time-lapse sequence of motile cells, this task consists in identifying and segmenting individual cell instances and in establishing their temporal relationships. Because cells frequently undergo division events, during which mother cells are split into two or even more daughter cells in case of abnormal divisions, linear oriented forests underrepresent such situations, making acyclic oriented graphs the preferred representation of cell lineages [34]. Cell tracking approaches can broadly be classified into two categories [41, 58]: *tracking by detection* [27, 45, 31, 6] and *tracking by model evolution* [18, 17, 35, 4]. The former paradigm, being followed also when tracking particles, involves two subsequent steps. First, a segmentation routine identifies and delineates individual cells in the entire time-lapse sequence separately for each frame. Second, the delineated cells are linked into tracks, mostly by optimizing a probabilistic objective function that evaluates the information from two successive frames, multiple successive frames, or even all frames at once. On the contrary, the latter paradigm solves both steps simultaneously, either under the instrumental assumption of unambiguous, spatiotemporal overlap between the corresponding cell regions using parametric or implicit active contour models, or without this limiting assumption using a Bayesian inference of dynamic models. Unsurprisingly, there is a recent rise of deep-learning-based workflows for tracking cells [46, 3, 28] in this field too.

Contributions

Inspired by the great success of PTC that was designed as a one-time event, the author has been co-organizing the Cell Tracking Challenge (CTC, <http://celltrackingchallenge.net>) since 2012, initially in close collaboration with the University of Navarra (Spain) and Erasmus University Medical Center (the Netherlands), and nowadays also with the Carlos III University of Madrid (Spain), Max Planck Institute of Molecular Cell Biology and Genetics (Dresden, Germany), and University of New South Wales (Australia). Being organized as five open competitions held under the auspices of the 2013, 2014, 2015, 2019, and 2020 IEEE International Symposium on Biomedical Imaging and running online since February 2017, it constitutes a renowned platform for objective and systematic comparison of cell tracking algorithms [39, 58]. Apart from a set of rigorous performance evaluation measures to assess detection, segmentation, and tracking accuracy, it offers a unique, highly heterogeneous, annotated repository of real and synthetic bioimage data, covering different imaging modalities (fluorescence, phase-contrast,

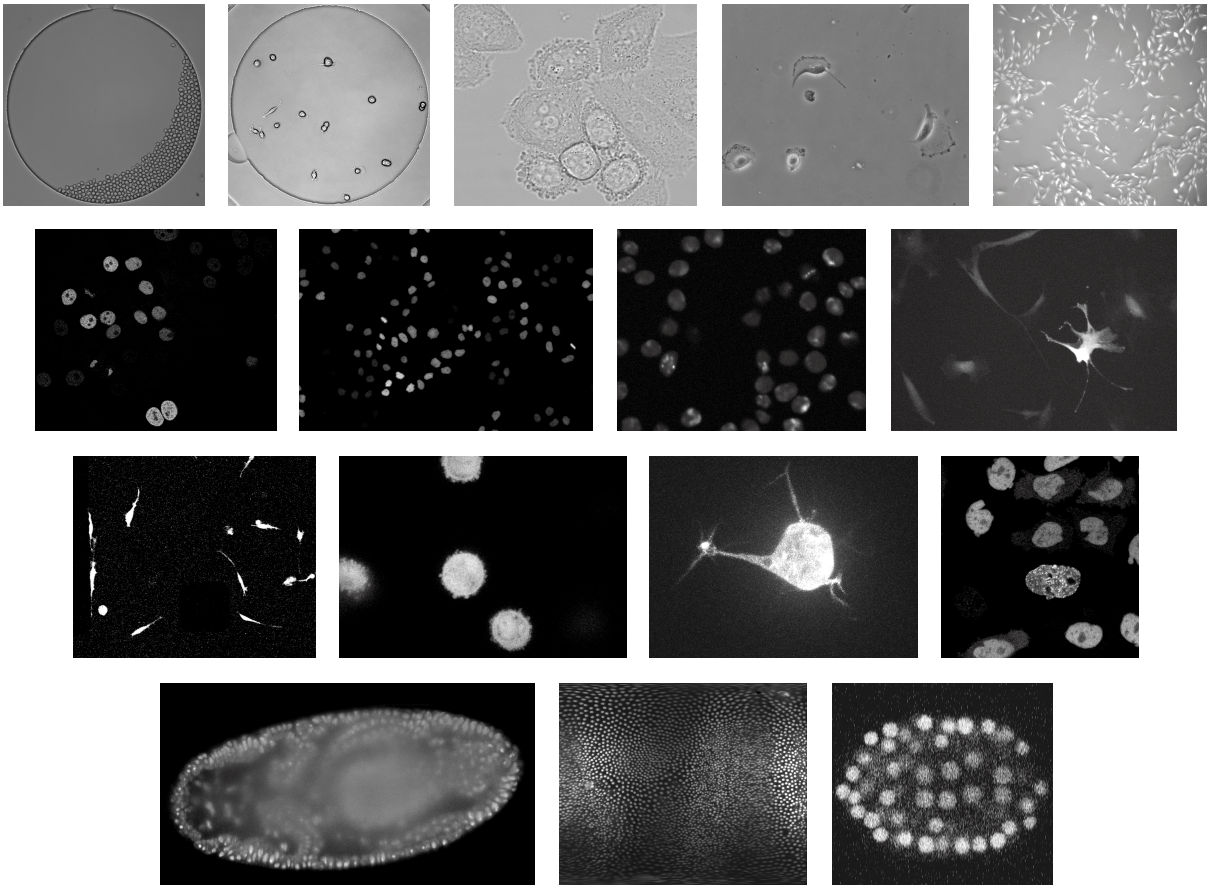


Figure 3.1: Samples of the Cell Tracking Challenge image data. The figure was inspired by [58] and extended accordingly by adding new samples of the datasets included in 2019 and 2020.

differential-interference-contrast, and brightfield microscopy), staining (nuclear and cellular), dimensionality (2D and 3D), and cell lines and organisms (*C. elegans*, *Drosophila Melanogaster*, and *Tribolium Castaneum*), as shown in Fig. 3.1. The key published outputs of this initiative, [39] and [58], lay down the principles of this challenge, summarize the results received within the first challenge edition [39] and over the first three challenge editions [58], and draw important practical conclusions for developers and users. As of April 2020, both papers together received more than 175 citations according to the Web of Science database and the number of objectively evaluated algorithms within the challenge has nearly doubled, from 21 algorithms submitted by 17 participating groups thoroughly analyzed in [58] to 50 algorithms submitted by 40 participating groups included in the online version of the challenge. This tremendous increase can be attributed not only to the recent boom of deep-learning methods that frequently populate top positions in the leaderboard (Fig. 3.4), but also to the possibility of evaluating segmentation results only in reaction to many requests received from the community in this regard. Indeed, since 2019 the Cell Tracking Challenge has simultaneously been running two benchmarks, Cell Tracking Benchmark and Cell Segmentation Benchmark, to objectively evaluate cell segmentation and tracking algorithms for time-lapse microscopy image data.

In contrast to widely used overlap-driven measures, such as the Dice or Jaccard coefficients,

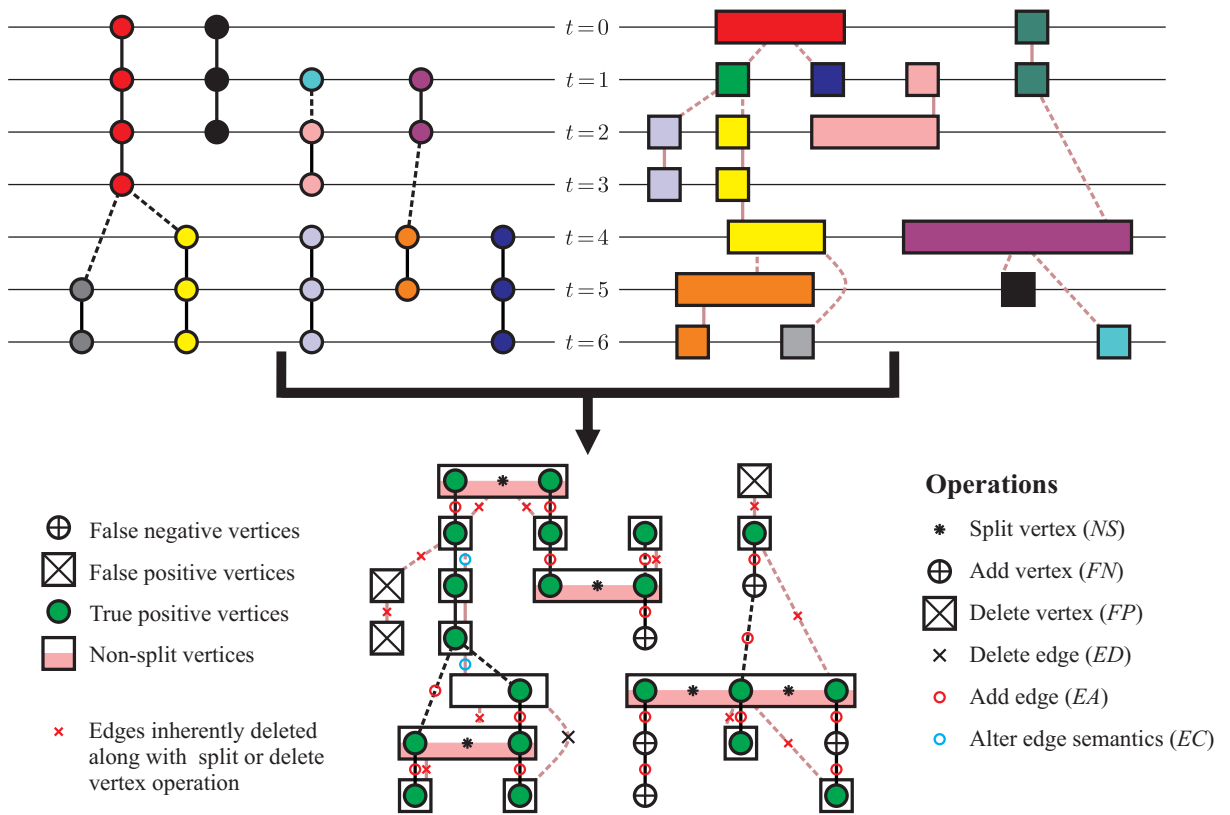


Figure 3.2: A schematic example of the Acyclic Oriented Graphs Matching measure calculation for a reference graph (top left) and an algorithm-generated graph (top right), with individual types of vertices and graph operations needed to transform the algorithm-generated graph to the reference graph being highlighted by different colors and symbols (bottom). The figure was reproduced from [34].

for evaluating cell segmentation performance, there was the lack of standardized measures for evaluating cell tracking performance in 2012, when the preparatory steps toward organizing the very first CTC edition were initiated. Therefore, we developed the Acyclic Oriented Graphs Matching (AOGM) measure [34] that penalizes all possible errors in cell tracking results and aggregates them into a single value, thus accounting for all important cellular events within a captured field of view, such as migration, division, death, and transit through it, within a single evaluation protocol (Fig. 3.2). The measure assesses the difficulty of transforming an algorithm-generated graph into a reference graph by calculating a weighted sum of the lowest number of allowed graph operations needed to make both graphs identical. Because the weights fairly reflect the effort needed to perform individual graph operations, the AOGM measure is flexible and universal. A different configuration of weights can serve purposes other than objectively comparing the performance of multiple cell tracking algorithms. It may also be useful to tune the parameters of individual modules involved in cell tracking algorithms under development, such as cell detection or cluster separation modules. Not being concentrated on a single, often application-limited aspect of cell tracking, it allows one to evaluate the tracking performance of any cell tracking algorithm irrespective of its nature because it works with its final output.

In [35], we developed a fast and robust approach to tracking cells in multidimensional fluorescence microscopy image data, which follows the tracking by model evolution paradigm. It consists in reducing the amount of noise and enhancing flow-like structures using a coherence-enhancing diffusion filter, and in detecting cell boundaries by minimizing the Chan–Vese model in the fast level set-like (FLS) and graph cut (GC) frameworks, both integrated with a topological prior to allow simultaneous tracking of multiple cells over time. By quantitatively as well as qualitatively comparing both frameworks, it has been shown that the GC framework is slightly more accurate and produces smoother boundaries (Fig. 3.3), but at the expense of substantially slower and more memory-demanding execution than the FLS framework. In March 2014, the FLS variant was objectively evaluated within the second Cell Tracking Challenge edition. As of April 2020, it has still been occupying the top position in terms of segmentation performance and the second position in terms of overall performance for the Fluo-N3DH-CHO dataset in both the Cell Segmentation Benchmark and Cell Tracking Benchmark (Fig. 3.4), being tagged as MU-CZ there. By contrast, the GC variant was exploited for quantifying cancer cell migration in collagen-Matrigel scaffolds [2], providing the solid ground for subsequent downstream analyses that revealed new insights on the mesenchymal and lobopodial migratory patterns of lung adenocarcinoma cells in reaction to the different amount of Matrigel in the composition of hydrogels. Indeed, in the pure collagen hydrogels, the cells showed clear polarization of their cell bodies with well-defined lamellipodia at their leading edges and rear ends, whereas they protruded numerous short-lifetime blebs along their surface after the addition of Matrigel into the hydrogels.

Articles in collection (in chronological order)

- M. Maška, O. Daněk, S. Garasa, A. Rouzaut, A. Muñoz-Barrutia, and C. Ortiz-de-Solórzano. Segmentation and shape tracking of whole fluorescent cells based on the Chan-Vese model. *IEEE Transactions on Medical Imaging*, 32(6):995–1006, 2013. [35]

Author’s contribution: method design, development, and implementation; evaluation and analysis of results; paper writing

- M. Maška, V. Ulman, D. Svoboda, P. Matula, P. Matula, C. Ederra, A. Urbiola, T. España, S. Venkatesan, D. M. W. Balak, P. Karas, T. Bolcková, M. Štreitová, C. Carthel, S. Coraluppi, N. Harder, K. Rohr, K. E. G. Magnusson, J. Jaldén, H. M. Blau, O. Dzyubachyk, P. Křížek, G. M. Hagen, D. Pastor-Escuredo, D. Jimenez-Carretero, M. J. Ledesma-Carbayo, A. Muñoz-Barrutia, E. Meijering, M. Kozubek, and C. Ortiz-de-Solórzano. A benchmark for comparison of cell tracking algorithms. *Bioinformatics*, 30(11):1609–1617, 2014. [39]

Author’s contribution: challenge co-organization; handling, evaluation, and analysis of submissions; implementation of evaluation and annotation software; supervision of annotations and creation of the consensual reference annotations; paper writing

- P. Matula, M. Maška, D. V. Sorokin, C. Ortiz-de-Solórzano, and M. Kozubek. Cell tracking accuracy measurement based on comparison of acyclic oriented graphs. *PLoS ONE*, 10(12):e0144959, 2015. [34]

Author’s contribution: method design, development, and implementation; evaluation and analysis of results; paper writing

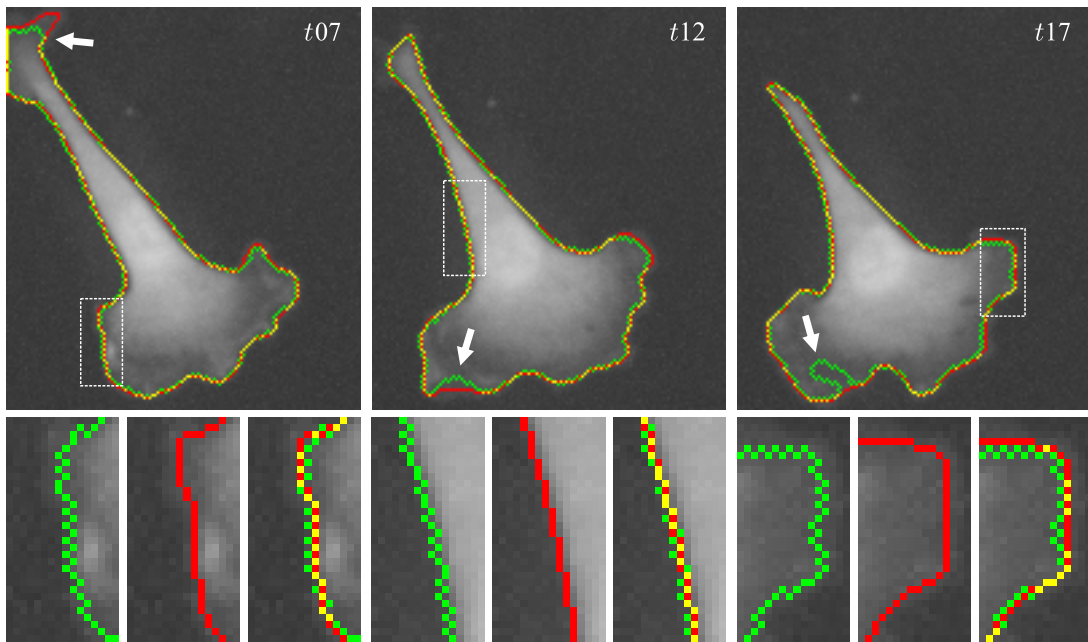


Figure 3.3: A comparison of the final contours obtained using both the fast level set-like (green) and graph cut (red) frameworks, with the contour intersections highlighted in yellow and the white rectangular areas zoomed in below. The white arrows identify foreground regions of low intensity levels in the close vicinity of the cell boundaries, which were undersegmented by the fast level set-like framework. The figure was reproduced from [35].

- M. Anguiano, C. Castilla, M. Maška, C. Ederra, R. Peláez, X. Morales, G. Muñoz-Arrieta, M. Mujika, M. Kozubek, A. Muñoz-Barrutia, A. Rouzaut, S. Arana, J. M. Garcia-Aznar, and C. Ortiz-de-Solorzano. Characterization of three-dimensional cancer cell migration in mixed collagen-Matrigel scaffolds using microfluidics and image analysis. *PLoS ONE*, 12(2):e0171417, 2017. [2]

Author's contribution: method development and implementation; visualization of results; paper editing

- V. Ulman, M. Maška, K. E. G. Magnusson, O. Ronneberger, C. Haubold, N. Harder, P. Matula, P. Matula, D. Svoboda, M. Radojevic, I. Smal, K. Rohr, J. Jaldén, H. M. Blau, O. Dzyubachyk, B. Lelieveldt, P. Xiao, Y. Li, S. Cho, A. C. Dufour, J.-C. Olivo-Marin, C. C. Reyes-Aldasoro, J. A. Solis-Lemus, R. Bensch, T. Brox, J. Stegmaier, R. Mikut, S. Wolf, F. A. Hamprecht, T. Esteves, P. Quelhas, Ö. Demirel, L. Malmström, F. Jug, P. Tomancak, E. Meijering, A. Muñoz-Barrutia, M. Kozubek, and C. Ortiz-de-Solórzano. An objective comparison of cell-tracking algorithms. *Nature Methods*, 14(12):1141–1152, 2017. [58]

Author's contribution: challenge co-organization and active participation; handling, evaluation, and analysis of submissions; implementation of evaluation and annotation software; supervision of annotations and creation of the consensual reference annotations; paper writing

	DIC-C2DH-Hela	Fluo-C2DL-MSC	Fluo-C3DH-H157	Fluo-C3DL-MDA231	Fluo-N2DH-GOWT1	Fluo-N2DL-Hela	Fluo-N3DH-CE	Fluo-N3DH-CHO	Fluo-N3DL-DRO	PhC-C2DH-U373	PhC-C2DL-P5C	Fluo-N2DH-SIM+	Fluo-N3DH-SIM+
OP	0.828	0.676 ⁽¹⁾	0.938 ⁽¹⁾	0.757 ⁽¹⁾	0.951 ⁽¹⁾	0.942 ⁽¹⁾	0.688 ⁽¹⁾	0.926 ⁽¹⁾	0.609 ⁽²⁾	0.951 ⁽¹⁾	0.804 ⁽¹⁾	0.878	0.848 ⁽¹⁾
	0.629 ⁽⁴⁾	0.636	0.885 ⁽¹⁾	0.745 ⁽¹⁾	0.902	0.940	0.601	0.912 ⁽¹⁾	0.285 ⁽¹⁾	0.896	0.772 ⁽¹⁾	0.874 ⁽¹⁾	0.798
	0.523 ⁽¹⁾	0.546	0.870 ⁽¹⁾	0.659 ⁽²⁾	0.902	0.901	0.507	0.906	0.219	0.886 ⁽³⁾	0.735	0.859	0.714 ⁽²⁾
SEG	0.776	0.590 ⁽¹⁾	0.888 ⁽¹⁾	0.631 ⁽¹⁾	0.927 ⁽¹⁾	0.903	0.479 ⁽¹⁾	0.917 ⁽¹⁾	0.561 ⁽²⁾	0.920	0.665	0.791 ⁽¹⁾	0.746 ⁽¹⁾
	0.460 ⁽⁴⁾	0.582	0.816 ⁽¹⁾	0.625 ⁽¹⁾	0.893	0.893 ⁽¹⁾	0.422	0.899 ⁽¹⁾	0.250	0.826	0.602 ⁽¹⁾	0.781	0.629 ⁽¹⁾
	0.293 ⁽¹⁾	0.465	0.773	0.504 ⁽⁴⁾	0.887	0.863	0.300	0.898 ⁽¹⁾	0.001	0.795 ⁽³⁾	0.572	0.770	0.593 ⁽⁴⁾
TRA	0.881	0.763 ⁽¹⁾	0.987 ⁽¹⁾	0.883 ⁽¹⁾	0.976 ⁽¹⁾	0.991 ⁽¹⁾	0.898 ⁽¹⁾	0.953 ⁽¹⁾	0.657 ⁽²⁾	0.981	0.943	0.975	0.967 ⁽¹⁾
	0.797 ⁽⁴⁾	0.691	0.976 ⁽¹⁾	0.865 ⁽¹⁾	0.925	0.986	0.781	0.935 ⁽¹⁾	0.438 ⁽¹⁾	0.977 ⁽³⁾	0.942 ⁽¹⁾	0.957 ⁽¹⁾	0.950 ⁽¹⁾
	0.752 ⁽¹⁾	0.645	0.954 ⁽¹⁾	0.830 ⁽¹⁾	0.916	0.982	0.713	0.914	0.320	0.965	0.898	0.948	0.835 ⁽²⁾

CUL-UK	CUNI-CZ	FR-Ro-GE +	HD-Har-GE
HD-Hau-GE +	IMCB-SG (1-2)	KIT-GE	LEID-NL
MU-CZ	NOTT-UK	PAST-FR	UZH-CH

	BF-C2DL-H5C	BF-C2DL-MuSC	DIC-C2DH-Hela	Fluo-C2DL-MSC	Fluo-C3DH-A549	Fluo-C3DH-H157	Fluo-C3DL-MDA231	Fluo-N2DH-GOWT1	Fluo-N2DL-Hela	Fluo-N3DH-CE	Fluo-N3DH-CHO	Fluo-N3DL-DRO	Fluo-N3DL-TRIC	PhC-C2DH-U373	PhC-C2DL-P5C	Fluo-C3DH-A549-SIM	Fluo-N2DH-SIM+	Fluo-N3DH-SIM+	
OP _{CTB}	0.868	0.835	0.909	0.759 ⁽¹⁾	0.916	0.938 ⁽¹⁾	0.757 ⁽¹⁾	0.951 ⁽¹⁾	0.953	0.808	0.926 ⁽¹⁾	0.617 ⁽²⁾	0.867 ⁽²⁾	0.785	0.951	0.843	0.920 ⁽¹⁾	0.896	0.848 ⁽¹⁾
	0.843 ⁽³⁾	0.800	0.904	0.740 ⁽¹⁾	0.913 ⁽¹⁾	0.885	0.745	0.934	0.944	0.803 ⁽¹⁾	0.912	0.429	0.787	0.698 ⁽²⁾	0.948	0.836	0.913	0.896	0.800
	0.840	0.770 ⁽³⁾	0.894	0.649	0.824	0.870	0.718	0.923	0.942	0.800	0.909	0.288	0.631	0.680	0.940	0.804	0.865	0.882 ⁽²⁾	0.798
SEG	0.757	0.702	0.863	0.645 ⁽¹⁾	0.831	0.888 ⁽¹⁾	0.632 ⁽¹⁾	0.927 ⁽¹⁾	0.919	0.729	0.917	0.567 ⁽²⁾	0.791 ⁽²⁾	0.684	0.924	0.720	0.840 ⁽¹⁾	0.825	0.746 ⁽¹⁾
	0.750	0.676	0.852	0.641 ⁽¹⁾	0.826 ⁽¹⁾	0.816	0.625	0.921	0.903	0.705	0.899 ⁽¹⁾	0.372	0.766	0.574 ⁽²⁾	0.922	0.715	0.827	0.822	0.668
	0.723 ⁽⁵⁾	0.628	0.834	0.617	0.647	0.789	0.616	0.909	0.902	0.662 ⁽¹⁾	0.898	0.251	0.562	0.573	0.920	0.682	0.730	0.807	0.629
TRA	0.978	0.971 ⁽³⁾	0.955	0.873 ⁽¹⁾	1.000	0.987 ⁽¹⁾	0.882 ⁽¹⁾	0.979	0.991 ⁽¹⁾	0.945 ⁽¹⁾	0.953 ⁽¹⁾	0.668 ⁽²⁾	0.942 ⁽²⁾	0.886	0.982	0.966	1.000	0.975	0.967
	0.964 ⁽⁵⁾	0.967	0.954	0.839 ⁽¹⁾	1.000	0.976	0.865	0.976 ⁽¹⁾	0.991	0.897	0.948	0.486	0.809	0.823 ⁽²⁾	0.981	0.959 ⁽¹⁾	1.000	0.973	0.950 ⁽¹⁾
	0.929	0.924	0.954	0.788	1.000	0.954	0.830	0.967 ⁽⁴⁾	0.989	0.895	0.935	0.438	0.699	0.788	0.979 ⁽⁴⁾	0.957	1.000	0.971	0.933

BGU-IL (1-4) +	CUL-UK	CUNI-CZ	CVUT-CZ +	FR-Ro-GE +	HD-Har-GE	CUNI-CZ	HIT-CN +	FR-Ro-GE +	LEID-NL	MU-CZ	KIT-Sch-GE +
FR-Ro-GE +	HD-Har-GE	HD-Hau-GE +	HIT-CN +	KTH-SE (1-5)	LEID-NL	MU-CZ	MU-Lux-CZ +	HD-Hau-GE +	PURD-US	MU-CZ	MU-US
ND-US +	PURD-US	RWTH-GE +	SZU-CN +	UCSB-US +	UP-PT	UVA-NL +	TUG-AT +	UCSB-US +	UP-PT	UVA-NL +	TUG-AT +

Figure 3.4: The top three best-performing algorithms within the Cell Tracking Benchmark as of February 2017 (upper) and of April 2020 (lower), with those involving a machine-learning-based step marked by plus signs. The results from the initial leaderboard, which are still listed in the current leaderboard, are marked by black dots.

Chapter 4

Filopodium Tracking

Filopodia are cell membrane protrusions governed by dynamic bundles of aligned actin filaments [33], acting as guidance sensors and promoters of cell locomotion in various physiological and pathological processes [53, 20, 21]. Nevertheless, their detailed biology has not been fully revealed yet [60, 22, 24]. Modern optical microscopy and fluorescent reporters have given researchers the opportunity to study filopodial behavior in diverse three-dimensional microenvironments at unprecedented spatiotemporal resolutions [44, 16]. In spite of recently emerging fully 3D filopodium segmentation and tracking approaches [10, 11], the previous lack of reliable and fully automatic bioimage analysis workflows for the quantification of filopodium-mediated processes in 3D+t bioimage data has impelled biologists to quantify 2D+t bioimage data solely in their daily practice [57, 5, 60, 22]. This simplification, consisting in selecting one optical section of the specimen or in transforming the acquired 3D stacks to their 2D maximum intensity projections, not only potentially results in erroneous information about the number of filopodia and their lengths due to their highly incoherent orientations [38], but it also forces developers to deal with unnatural scenarios, such as crossing filopodia [60].

Contributions

Being impressed by the dynamic changes of filopodial protrusions over time and their different morphology across cell phenotypes (Fig. 4.1a-c), the author has been working on the tracking of filopodial protrusions in 3D+t fluorescence microscopy image data since 2012. Shortly before the end of his postdoctoral research stay at the Center for Applied Medical Research (University of Navarra, Spain), a first fully automatic approach to quantitatively analyzing filopodial protrusions of migrating cells in 3D+t fluorescence microscopy image data was introduced [37]. Although it helped us to successfully describe the different morphology of three distinct lung cancer cell phenotypes, its ability to accurately segment branching filopodia was limited due to the single-scale nature of the steerable, Hessian-based ridge detector employed and any information on the temporal evolution of individual filopodia was missing.

Between 2016 and 2018, the author was awarded a grant from the Czech Science Foundation, which initiated a huge step toward robust fully 3D filopodium segmentation and tracking in time-lapse fluorescence microscopy. With several proof-of-concept papers published at prestigious international conferences [55, 10, 47], the most noticeable results achieved in the project were published in [56, 61, 11, 38], establishing a comprehensive resource for quantitative analy-

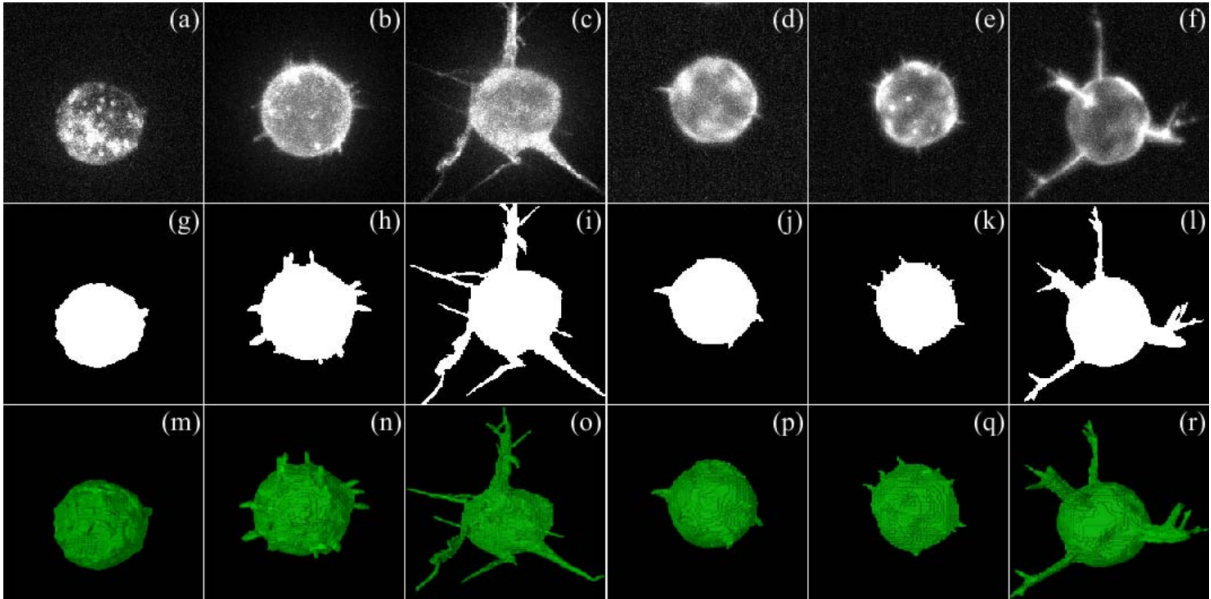


Figure 4.1: Maximum intensity projections along the axial direction of contrast-enhanced image data of (a-c) real and (d-f) synthetic filopodial cells, accompanied by (g-l) segmentation mask projections and (m-r) 3D renderings. The figure was reproduced from [11].

ses of 3D+t sequences of filopodial cells, the development of fully 3D filopodium segmentation and tracking methods, and objective benchmarking of their performance.

FiloGen [56] is a flexible simulation system capable of generating 3D+t sequences of motile cells with filopodia of user-controlled structural and temporal attributes, such as the number, thickness, length, level of branching, and lifetime of filopodia, accompanied by inherently generated reference annotations. The system consists of three globally synchronized modules, responsible for stochastic simulations of filopodial evolution, simultaneous deformations of the entire cell with filopodia using linear elasticity, and the synthesis of realistic, time-coherent cell texture utilizing clouds of simulated fluorescent particles in the spatiotemporal domain, the content of which is periodically submitted to a virtual microscope [59]. A high level of structural, visual, and quantitative similarity of the FiloGen-generated bioimage data (Fig. 4.1d-f) to its real counterparts supported the inclusion of new synthetic bioimage data into the CTC dataset repository, being tagged as Fluo-C3DH-A549-SIM, and advanced the development of our deep-learning-based pipeline for fully 3D filopodium segmentation and tracking [10, 11].

Apart from making FiloGen publicly available in the form of a pre-configured virtual machine, it was integrated into CytoPacq [61], initiating the addition of new features to fully exploit its capabilities. CytoPacq is a modular web-interface specifically developed for generating synthetic benchmark datasets of various cytology-centric 3D digital phantoms, supporting different configurations of the optical system and acquisition devices, including time-lapse imaging. First, it allows even unexperienced users to conveniently configure the whole simulation process by controlling the most important parameters only and by navigating their steps using informative tooltips, instead of laboriously compiling and installing individual simulation system modules and third-party libraries on their own. Second, it allows one to generate not only individual 3D+t sequences of different synthetic filopodial cells in each simulation run,

but also a set of such sequences of the same synthetic filopodial cell with varying signal-to-noise and anisotropy ratios at once, which are both well-known factors that often influence the performance of segmentation and tracking algorithms. This new feature greatly facilitated the synthetic image data preparation for the quantitative analyses carried out in [11, 38].

In [11], we introduced a pioneering approach to robustly analyzing the 3D morphology and dynamics of arbitrarily oriented filopodial structures for cells embedded in three-dimensional microenvironments of high physiological relevance, having the ability to generalize to varying cell phenotypes, signal-to-noise ratios, and imaging systems (Fig. 4.1g-r). It employs two convolutional neural networks trained using real and synthetic image data to segment the whole cell volumes with highly heterogeneous fluorescence intensity levels and to detect individual filopodial protrusions, followed by a constrained nearest-neighbor tracker of filopodial tips to obtain valuable information about the spatiotemporal evolution of individual protrusions. The developed deep-learning-based workflow provides both quantitative as well as qualitative advantages compared to the baseline, machine-learning-free method based on the minimization of the Chan-Vese model [35], which has been deemed especially appropriate for the tracking of cells imaged at high spatiotemporal resolutions [58].

In [38], we introduced a new benchmark dataset, FiloData3D, designed for in-depth performance assessments of fully 3D filopodium segmentation and tracking algorithms. It consists of 180 synthetic, fully annotated, 3D time-lapse sequences of single lung cancer cells, combining different cell shapes, signal-to-noise ratios, and anisotropy ratios (Fig. 4.2). Using FiloData3D, it has been shown that the basic quantitative features, the number of filopodia and their length, are significantly underestimated when being extracted using traditional 2D-projection-oriented and 2D-selection-oriented protocols that prevail in daily practice [57, 5, 60, 22], calling for a procedural change in filopodial analyses of 3D+t bioimage data.

Articles in collection (in chronological order)

- M. Maška, X. Morales, A. Muñoz-Barrutia, A. Rouzaut, and C. Ortiz-de-Solórzano. Automatic quantification of filopodia-based cell migration. In *Proceedings of the 10th IEEE International Symposium on Biomedical Imaging*, pages 668–671, 2013. [37]

Author's contribution: method design, development, and implementation; evaluation and analysis of results; paper writing

- D. V. Sorokin, I. Peterlík, V. Ulman, D. Svoboda, T. Nečasová, K. Morgaenko, L. Eiselleová, L. Tesařová, and M. Maška. FiloGen: A model-based generator of synthetic 3-D time-lapse sequences of single motile cells with growing and branching filopodia. *IEEE Transactions on Medical Imaging*, 37(12):2630–2641, 2018. [56]

Author's contribution: simulation system design; validation of filopodial dynamics; paper writing; supervision of the work

- C. Castilla, M. Maška, D. V. Sorokin, E. Meijering, and C. Ortiz-de-Solórzano. 3-D quantification of filopodia in motile cancer cells. *IEEE Transactions on Medical Imaging*, 38(3):862–872, 2019. [11]

Author's contribution: method design; preparation of synthetic image data; evaluation and analysis of results; paper writing; co-supervision of the work

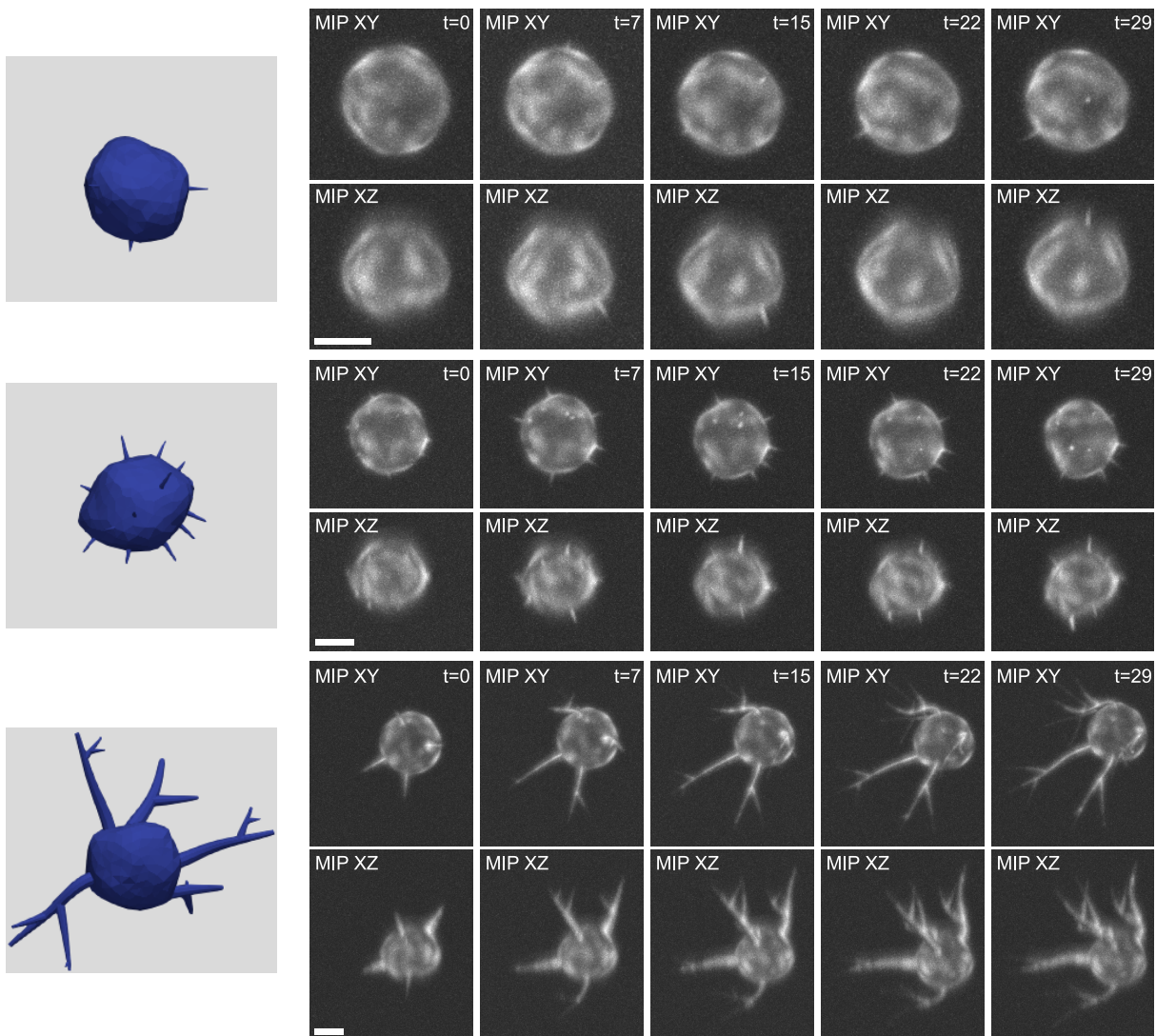


Figure 4.2: Samples of the FiloData3D image data. Right: A rendered filopodial cell geometry. Left: Maximum intensity projections of contrast-enhanced, isotropic image data with a medium signal-to-noise ratio. The scale bars correspond to $5\ \mu\text{m}$. The figure was reproduced from [38].

- D. Wiesner, D. Svoboda, M. Maška, and M. Kozubek. CytoPacq: A web-interface for simulating multi-dimensional cell imaging. *Bioinformatics*, 35(21):4531–4533, 2019. [61]
Author's contribution: benchmark mode design; paper editing; co-supervision of the work
- M. Maška, T. Nečasová, D. Wiesner, D. Sorokin, I. Peterlík, V. Ulman, and D. Svoboda. Toward robust fully 3D filopodium segmentation and tracking in time-lapse fluorescence microscopy. In *Proceedings of the 26th IEEE International Conference on Image Processing*, pages 819–823, 2019. [38]
Author's contribution: preparation of image data; evaluation and analysis of results; paper writing; supervision of the work

Chapter 5

Conclusion

In this commentary, the author has comprehensively summarized his concerted efforts made to develop robust and automatic workflows for tracking particles, cells, and filopodial protrusions in multidimensional bioimage data. The full versions of the representative collection of papers published by the author on this research topic are available next, but only in the printed version of this thesis to avoid copyright infringement.

Despite never-ending progress in the development of bioimage tracking workflows highly stimulated by ever-growing massive amounts of multidimensional bioimage data, their generalization across multiple imaging modalities, scales, and target domains is still a distant dream. Objectively evaluating cutting-edge bioimage trackers for more than half a decade, the author has been witnessing the current lack of methods that produce reliable and stable results over highly heterogeneous datasets, including high-resolution and low-resolution, time-lapse fluorescence and label-free microscopy image data of particles and cells with and without visible cellular protrusions acquired in both 2D and 3D. Unifying the point-centric and region-centric performance evaluation protocols into a single framework might be one of the game-changers on this challenging hunt for generalization. Such a unified framework would not only allow one to straightforwardly assess the performance of the state-of-the-art, single-domain trackers within other target domains, but more importantly it may also help to gather the particle, cell, and filopodium tracking communities, thus addressing different bioimage tracking challenges with their concerted efforts. A valuable source of inspiration can be found in [7] where several cell nucleus segmentation routines capable of generalizing across multiple imaging modalities and scales were introduced. However, it remains unexplored whether these ideas are also viable in time-lapse bioimage data and for objects with highly irregular shapes, compared to the static images of cell nuclei with roughly compact shapes.

Bibliography

- [1] R. Ananthkrishnan and A. Ehrlicher. The forces behind cell movement. *International Journal of Biological Sciences*, 3(5):303–317, 2007.
- [2] M. Anguiano, C. Castilla, M. Maška, C. Ederra, R. Peláez, X. Morales, G. Muñoz-Arrieta, M. Mujika, M. Kozubek, A. Muñoz-Barrutia, A. Rouzaut, S. Arana, J. M. Garcia-Aznar, and C. Ortiz-de-Solorzano. Characterization of three-dimensional cancer cell migration in mixed collagen-Matrigel scaffolds using microfluidics and image analysis. *PLoS ONE*, 12(2):e0171417, 2017.
- [3] A. Arbelle and T. R. Raviv. Microscopy cell segmentation via convolutional LSTM networks. In *Proceedings of the 16th IEEE International Symposium on Biomedical Imaging*, pages 1008–1012, 2019.
- [4] A. Arbelle, J. Reyes, J.-Y. Chen, G. Lahav, and T. R. Raviv. A probabilistic approach to joint cell tracking and segmentation in high-throughput microscopy videos. *Medical Image Analysis*, 47(7):140–152, 2018.
- [5] D. J. Barry, C. H. Durkin, J. V. Abella, and M. Way. Open source software for quantification of cell migration, protrusions, and fluorescence intensities. *Journal of Cell Biology*, 209(1):163–180, 2015.
- [6] R. Bensch and O. Ronneberger. Cell segmentation and tracking in phase contrast images using graph cut with asymmetric boundary costs. In *Proceedings of the 12th IEEE International Symposium on Biomedical Imaging*, pages 1220–1223, 2015.
- [7] J. C. Caicedo, A. Goodman, K. W. Karhohs, B. A. Cimini, J. Ackerman, M. Haghghi, C. Heng, T. Becker, M. Doan, C. McQuin, M. Rohban, S. Singh, and A. E. Carpenter. Nucleus segmentation across imaging experiments: The 2018 Data Science Bowl. *Nature Methods*, 16(10):1247–1253, 2019.
- [8] A. Cardona and P. Tomancak. Current challenges in open-source bioimage informatics. *Nature Methods*, 9(7):661–665, 2012.
- [9] A. E. Carpenter, L. Kametsky, and K. W. Eliceiri. A call for bioimaging software usability. *Nature Methods*, 9(7):666–670, 2012.
- [10] C. Castilla, M. Maška, D. V. Sorokin, E. Meijering, and C. Ortiz-de-Solorzano. Segmentation of actin-stained 3D fluorescent cells with filopodial protrusions using convolutional neural networks. In *Proceedings of the 15th IEEE International Symposium on Biomedical Imaging*, pages 413–417, 2018.

- [11] C. Castilla, M. Maška, D. V. Sorokin, E. Meijering, and C. Ortiz-de-Solórzano. 3-D quantification of filopodia in motile cancer cells. *IEEE Transactions on Medical Imaging*, 38(3):862–872, 2019.
- [12] K. Celler, G. P. van Wezzel, and J. Willemsse. Single particle tracking of dynamically localizing TatA complexes in *Streptomyces coelicolor*. *Biochemical and Biophysical Research Communications*, 438(1):38–42, 2013.
- [13] N. Chenouard, I. Bloch, and J.-C. Olivo-Marin. Multiple hypothesis tracking for cluttered biological image sequences. *IEEE Transactions on Pattern Analysis and Machine Intelligence*, 35(11):2736–2750, 2013.
- [14] N. Chenouard, I. Smal, F. de Chaumont, M. Maška, I. F. Sbalzarini, Y. Gong, J. Cardinale, C. Carthel, S. Coraluppi, M. Winter, A. R. Cohen, W. J. Godinez, K. Rohr, Y. Kalaidzidis, L. Liang, J. Duncan, H. Shen, Y. Xu, K. E. G. Magnusson, J. Jaldén, H. M. Blau, P. Paul-Gilloteaux, P. Roudot, C. Kervrann, F. Waharte, J.-Y. Tinevez, S. L. Shorte, J. Willemsse, K. Celler, G. P. van Wezel, H.-W. Dan, Y.-S. Tsai, C. Ortiz-de-Solórzano, J.-C. Olivo-Marin, and E. Meijering. Objective comparison of particle tracking methods. *Nature Methods*, 11(3):281–289, 2014.
- [15] D. L. Coutu and T. Schroeder. Probing cellular processes by long-term live imaging—historic problems and current solutions. *Journal of Cell Science*, 126(17):3805–3815, 2013.
- [16] M. K. Driscoll and G. Danuser. Quantifying modes of 3D cell migration. *Trends in Cell Biology*, 25(12):749–759, 2015.
- [17] A. Dufour, R. Thibeaux, E. Labruyère, N. Guillén, and J.-C. Olivo-Marin. 3-D active meshes: Fast discrete deformable models for cell tracking in 3-D time-lapse microscopy. *IEEE Transactions on Image Processing*, 20(7):1925–1937, 2011.
- [18] O. Dzyubachyk, W. A. van Cappellen, J. Essers, W. J. Niessen, and E. Meijering. Advanced level-set-based cell tracking in time-lapse fluorescence microscopy. *IEEE Transactions on Medical Imaging*, 29(3):852–867, 2010.
- [19] W. J. Godinez and K. Rohr. Tracking multiple particles in fluorescence time-lapse microscopy images via probabilistic data association. *IEEE Transactions on Medical Imaging*, 34(2):415–432, 2015.
- [20] A. Haeger et al. Collective cell migration: Guidance principles and hierarchies. *Trends in Cell Biology*, 25(9):556–566, 2015.
- [21] G. Jacquemet, H. Hamidi, and J. Ivaska. Filopodia in cell adhesion, 3D migration and cancer cell invasion. *Current Opinion in Cell Biology*, 31(10):23–31, 2015.
- [22] G. Jacquemet, I. Paatero, A. F. Carisey, A. Padzik, J. S. Orange, H. Hamidi, and J. Ivaska. FiloQuant reveals increased filopodia density during breast cancer progression. *Journal of Cell Biology*, 216(10):3387–3403, 2017.
- [23] K. Jaqaman, D. Loerke, M. Mettlen, H. Kuwata, S. Grinstein, S. L. Schmid, and G. Danuser. Robust single-particle tracking in live-cell time-lapse sequences. *Nature Methods*, 5(8):695–702, 2008.

- [24] I. K. Jarsch, J. R. Gadsby, A. Nuccitelli, J. Mason, H. Shimo, L. Pilloux, B. Marzook, C. M. Mulvey, U. Dobramysl, C. R. Bradshaw, K. S. Lilley, R. D. Hayward, T. J. Vaughan, C. L. Dobson, and J. L. Gallop. A direct role for SNX9 in the biogenesis of filopodia. *Journal of Cell Biology*, 219(4):e201909178, 2020.
- [25] M. Kozubek. Challenges and benchmarks in bioimage analysis. In *Advances in Anatomy, Embryology and Cell Biology*, volume 219, pages 231–262. Springer, Cham, 2016.
- [26] Y. LeCun, Y. Bengio, and G. Hinton. Deep learning. *Nature*, 521(6):436–444, 2015.
- [27] F. Li, X. Zhou, J. Ma, and S. T. C. Wong. Multiple nuclei tracking using integer programming for quantitative cancer cell cycle analysis. *IEEE Transactions on Medical Imaging*, 29(1):96–105, 2010.
- [28] F. Lux and P. Matula. DIC image segmentation of dense cell populations by combining deep learning and watershed. In *Proceedings of the 16th IEEE International Symposium on Biomedical Imaging*, pages 236–239, 2019.
- [29] Y. Ma, X. Wand H. Liu, L. Wei, and L. Xiao. Recent advances in optical microscopic methods for single-particle tracking in biological samples. *Analytical and Bioanalytical Chemistry*, 411(2):4445–4463, 2019.
- [30] K. E. G. Magnusson and J. Jaldén. Tracking of non-Brownian particles using the Viterbi algorithm. In *Proceedings of the 12th IEEE International Symposium on Biomedical Imaging*, pages 380–384, 2015.
- [31] K. E. G. Magnusson, J. Jaldén, P. M. Gilbert, and H. M. Blau. Global linking of cell tracks using the Viterbi algorithm. *IEEE Transactions on Medical Imaging*, 34(4):911–929, 2015.
- [32] L. Maier-Hein, M. Eisenmann, A. Reinke, S. Onogu, M. Stankovic, P. Scholz, T. Arbel, H Bogunovic, A. Bradley, A. Carass, C. Feldmann, A. Frangi, P. M. Full, B. van Ginneken, A. Hanbury, K. Honauer, M. Kozubek, B. A. Landman, K. März, O. Maier, K. Maier-Hein, B. H. Menze, H. Müller, P. F. Neher, W. Niessen, N. Rajpoot, G. C. Sharp, K. Sirinukunwatana, S. Speidel, C. Stock, D. Stoyanov, A. A. Taha, F. van der Sommen, C.-W. Wang, M.-A. Weber, G. Zheng, P. Jannin, and A. Kopp-Schneider. Why rankings of biomedical image analysis competitions should be interpreted with care. *Nature Communications*, 9(12):5217, 2018.
- [33] P. K. Mattila and P. Lappalainen. Filopodia: Molecular architecture and cellular functions. *Nature Reviews Molecular Cell Biology*, 9(6):446–454, 2008.
- [34] P. Matula, M. Maška, D. V. Sorokin, C. Ortiz-de-Solórzano, and M. Kozubek. Cell tracking accuracy measurement based on comparison of acyclic oriented graphs. *PLoS ONE*, 10(12):e0144959, 2015.
- [35] M. Maška, O. Daněk, S. Garasa, A. Rouzaut, A. Muñoz-Barrutia, and C. Ortiz-de-Solórzano. Segmentation and shape tracking of whole fluorescent cells based on the Chan-Vese model. *IEEE Transactions on Medical Imaging*, 32(6):995–1006, 2013.

- [36] M. Maška and P. Matula. Particle tracking accuracy measurement based on comparison of linear oriented forests. In *IEEE International Conference on Computer Vision Workshops*, pages 11–17, 2017.
- [37] M. Maška, X. Morales, A. Muñoz-Barrutia, A. Rouzaut, and C. Ortiz-de-Solórzano. Automatic quantification of filopodia-based cell migration. In *Proceedings of the 10th IEEE International Symposium on Biomedical Imaging*, pages 668–671, 2013.
- [38] M. Maška, T. Nečasová, D. Wiesner, D. Sorokin, I. Peterlík, V. Ulman, and D. Svoboda. Toward robust fully 3D filopodium segmentation and tracking in time-lapse fluorescence microscopy. In *Proceedings of the 26th IEEE International Conference on Image Processing*, pages 819–823, 2019.
- [39] M. Maška, V. Ulman, D. Svoboda, P. Matula, P. Matula, C. Ederra, A. Urbiola, T. España, S. Venkatesan, D. M. W. Balak, P. Karas, T. Bolcková, M. Štreitová, C. Carthel, S. Coraluppi, N. Harder, K. Rohr, K. E. G. Magnusson, J. Jaldén, H. M. Blau, O. Dzyubachyk, P. Křížek, G. M. Hagen, D. Pastor-Escuredo, D. Jimenez-Carretero, M. J. Ledesma-Carbayo, A. Muñoz-Barrutia, E. Meijering, M. Kozubek, and C. Ortiz-de-Solórzano. A benchmark for comparison of cell tracking algorithms. *Bioinformatics*, 30(11):1609–1617, 2014.
- [40] E. Meijering, A. E. Carpenter, H. Peng, F. A. Hamprecht, and J.-C. Olivo-Marin. Imaging the future of bioimage analysis. *Nature Biotechnology*, 34(12):1250–1255, 2016.
- [41] E. Meijering, O. Dzyubachyk, I. Smal, and W. A. Cappelletti. Tracking in cell and developmental biology. *Seminars in Cell and Developmental Biology*, 20(8):894–902, 2009.
- [42] E. Moen, D. Bannon, T. Kudo, W. Graf, M. Covert, and D. van Valen. Deep learning for cellular image analysis. *Nature Methods*, 16(12):1233–1246, 2019.
- [43] J. M. Newby, A. M. Schaefer, P. T. Lee, M. G. Forest, and S. K. Lai. Convolutional neural networks automate detection for tracking of submicron-scale particles in 2D and 3D. *Proceedings of the National Academy of Sciences of the United States of America*, 115(36):9026–9031, 2018.
- [44] C. Ortiz-de-Solórzano, A. Muñoz-Barrutia, E. Meijering, and M. Kozubek. Toward a morphodynamic model of the cell. *Signal Processing Magazine*, 32(1):20–29, 2015.
- [45] D. Padfield, J. Rittscher, and B. Roysam. Coupled minimum-cost flow cell tracking for high-throughput quantitative analysis. *Medical Image Analysis*, 15(1):650–668, 2011.
- [46] C. Payer, D. Štern, M. Feiner, H. Bischof, and M. Urschler. Segmenting and tracking cell instances with cosine embeddings and recurrent hourglass networks. *Medical Image Analysis*, 57(10):106–119, 2019.
- [47] I. Peterlík, D. Svoboda, V. Ulman, D. V Sorokin, and M. Maška. Model-based generation of synthetic 3D time-lapse sequences of multiple mutually interacting motile cells with filopodia. In *Simulation and Synthesis in Medical Imaging*, pages 71–79, 2018.
- [48] A. Reinke, M. Eisenmann, S. Onogur, M. Stankovic, P. Scholz, P. M. Full, H. Bogunovic, B. A. Landman, O. Maier, B. Menze, G. C. Sharp, K. Sirinukunwattana, S. Speidel, F. van

- der Sommen, G. Zheng, H. Müller, M. Kozubek, T. Arbel, A. P. Bradley, P. Jannin, A. Kopp-Schneider, and L. Maier-Hein. How to exploit weaknesses in biomedical challenge design and organization. In *Proceedings of the 21st International Conference on Medical Image Computing and Computer-Assisted Intervention*, pages 388–395, 2018.
- [49] D. Sage, H. Kirshner, T. Pengo, N. Stuurman, J. Min, S. Manley, and M. Unser. Quantitative evaluation of software packages for single-molecule localization microscopy. *Nature Methods*, 12(8):717–724, 2015.
- [50] D. Sage, T.-A. Pham, H. Babcock, T. Lukes, T. Pengo, J. Chao, R. Velmurugan, A. Herbert, A. Agrawal, S. Colabrese, A. Wheeler, A. Archett, B. Rieger, R. Ober, G. M. Hagen, J.-B. Sibarita, J. Ries, R. Henriques, M. Unser, and S. Holden. Super-resolution fight club: Assessment of 2D and 3D single-molecule localization microscopy software. *Nature Methods*, 16(4):387–395, 2019.
- [51] I. Sgouralis, A. Nebenführ, and V. Maroulas. A Bayesian topological framework for the identification and reconstruction of subcellular motion. *SIAM Journal of Image Sciences*, 10(2):871–899, 2017.
- [52] H. Shen, L. J. Tauzin, R. Baiyasi, W. Wang, N. Moringo, B. Shuang, and C. F. Landes. Single particle tracking: From theory to biophysical applications. *Chemical Reviews*, 117(11):7331–7376, 2017.
- [53] T. Shibue, M. W. Brooks, M. F. Inan, F. Reinhardt, and R. A. Weinberg. The outgrowth of micrometastases is enabled by the formation of filopodium-like protrusions. *Cancer Discovery*, 2(8):706–721, 2012.
- [54] I. Smal, Y. Yao, N. Galjart, and E. Meijering. Facilitating data association in particle tracking using autoencoding and score matching. In *Proceedings of the 16th IEEE International Symposium on Biomedical Imaging*, pages 1523–1526, 2019.
- [55] D. V. Sorokin, I. Peterlík, V. Ulman, D. Svoboda, and M. Maška. Model-based generation of synthetic 3D time-lapse sequences of motile cells with growing filopodia. In *Proceedings of the 14th IEEE International Symposium on Biomedical Imaging*, pages 822–826, 2017.
- [56] D. V. Sorokin, I. Peterlík, V. Ulman, D. Svoboda, T. Nečasová, K. Morgaenko, L. Eiselleová, L. Tesařová, and M. Maška. FiloGen: A model-based generator of synthetic 3-D time-lapse sequences of single motile cells with growing and branching filopodia. *IEEE Transactions on Medical Imaging*, 37(12):2630–2641, 2018.
- [57] D. Tsygankov, C. G. Bilancia, E. A. Vitriol, K. M. Hahn, M. Peifer, and T. C. Elston. Cell-Geo: A computational platform for the analysis of shape changes in cells with complex geometries. *Journal of Cell Biology*, 204(3):443–460, 2014.
- [58] V. Ulman, M. Maška, K. E. G. Magnusson, O. Ronneberger, C. Haubold, N. Harder, P. Matula, P. Matula, D. Svoboda, M. Radojevic, I. Smal, K. Rohr, J. Jaldén, H. M. Blau, O. Dzyubachyk, B. Lelieveldt, P. Xiao, Y. Li, S. Cho, A. C. Dufour, J.-C. Olivo-Marin, C. C. Reyes-Aldasoro, J. A. Solis-Lemus, R. Bensch, T. Brox, J. Stegmaier, R. Mikut, S. Wolf, F. A. Hamprecht, T. Esteves, P. Quelhas, Ö. Demirel, L. Malmström, F. Jug, P. Tomancak, E. Meijering,

- A. Muñoz-Barrutia, M. Kozubek, and C. Ortiz-de-Solórzano. An objective comparison of cell-tracking algorithms. *Nature Methods*, 14(12):1141–1152, 2017.
- [59] V. Ulman, D. Svoboda, M. Nykter, M. Kozubek, and P. Ruusuvuori. Virtual cell imaging: A review on simulation methods employed in image cytometry. *Cytometry Part A*, 89(12):1057–1072, 2016.
- [60] V. Urbančič, R. Butler, B. Richier, M. Peter, J. Mason, F. J. Livesey, C. E. Holt, and J. L. Gallop. Filopodyan: An open-source pipeline for the analysis of filopodia. *Journal of Cell Biology*, 216(10):3405–3422, 2017.
- [61] D. Wiesner, D. Svoboda, M. Maška, and M. Kozubek. CytoPacq: A web-interface for simulating multi-dimensional cell imaging. *Bioinformatics*, 35(21):4531–4533, 2019.
- [62] T. Wollmann, C. Ritter, J. N. Dohrke, J.-Y. Lee, R. Bartenschlager, and K. Rohr. Detnet: Deep neural network for particle detection in fluorescence microscopy images. In *Proceedings of the 16th IEEE International Symposium on Biomedical Imaging*, pages 517–520, 2019.
- [63] Y. Yao, I. Smal, and E. Meijering. Deep neural networks for data association in particle tracking. In *Proceedings of the 15th IEEE International Symposium on Biomedical Imaging*, pages 458–461, 2018.